

## Electron transport through two-dimensional quantum wires with flanges

S. Midgley and J. B. Wang

*Department of Physics, The University of Western Australia, Perth 6907, Australia*

(Received 10 May 2000; revised manuscript received 5 September 2000; published 28 September 2001)

We report a detailed theoretical study on electron transport through a quantum wire connected to the source and drain by flanges. Our results show that the connection flange angle affects significantly the electron transmission through the wire. Resonant reflection and trapping are observed in our calculations. The optimal flange angle that allows maximum transmission corresponds to this resonance condition, which is around  $18^\circ$  and is essentially independent of the width or length of the wire. This angle changes by a few degrees when the initial energy, the energy spread of the wave packet, or the length of the flange changes. Such a finding can be used to assist the design of high-conductance quantum wires.

DOI: 10.1103/PhysRevB.64.153304

PACS number(s): 73.23.Ad, 73.23.Hk

The fabrication of nanostructures is currently underway at many research institutes around the world, with the areas of study ranging from geometric considerations to quantum chaos. As the fabrication of these structures becomes easier and their properties understood, they will start to become more important in the electronic industry. If the time line described by Sohn<sup>1</sup> is used as a guide, mainstream silicon chip manufactures will be reaching the nanometer scale in approximately 10 years time.

Much of the research undertaken thus far has been concerned with the actual manufacture of these devices and observing fundamental quantum phenomena (for example, quantum tunneling and electron blockade). Recent efforts have started to focus on using these structures to build usable computing devices (for example, the quantum transistor and single-electron devices) and how these structures will interact with each other and their environment. For an overview of the field see Refs. 2 and 3.

Due to the quantum nature of the electron in these devices, the geometric shape and layout becomes increasingly important. This paper demonstrates how the connection of a quantum wire to its environment and the shape of that connection can affect the propagation of a single electron through the device. From this study an optimal flange angle is obtained, which allows maximum transmission of the electrons. An interpretation of the physics at work is also presented.

Although many reported experiments have flanges connecting the source and drain to the nanodevices,<sup>4–8</sup> experimentally changing flange angles is difficult and very costly because this would require a new device to be constructed for each angle. Consequently, no known experiment has been performed that varies the flange angle while keeping the other aspects of the device constant. The effect of the flanges on the operation of these devices is usually considered as an artifact of device construction, but this has not been studied in detail.

Theoretical study of connecting quantum wires to the source and drain smoothly or via a flange, as discussed in this paper, has partially been investigated by Szafer and

Stone<sup>9</sup> and Rasavy.<sup>10</sup> Szafer and Stone used a linear flange to connect different width wires  $W$  and  $W'$ , and compared the results obtained to those with no flanges. No detailed analysis of the flange profiles was undertaken. Rasavy studied two- and three-dimensional quantum wires connected smoothly to leads. Their results gave the transmission coefficients for two different quantum wire widths as a function of effective wave number, but they did not study the effect of changing the flange angles on the electron transport through quantum wires.

The study undertaken in this paper computes the transmission coefficient and conductance of electron transport through quantum wires for different flange angles. The results obtained provide theoretical guidance to the actual design of high-conductance quantum wires. The general procedure used to study electron transport in nanostructures is to solve directly the time-dependent Schrödinger equation with the appropriate confinement potential. The theoretical formulation and computational method has been reported in detail elsewhere.<sup>11</sup> For completeness, a brief description is given below.

The time-dependent Schrödinger equation for describing two-dimensional electron transport in nanostructures with an external potential is given as

$$i(\partial\psi(x,y,t)/\partial t) = \mathcal{H}\psi(x,y,t), \quad (1)$$

with a general solution

$$\psi(x,y,t) = \exp(-i\mathcal{H}t)\psi(x,y,0), \quad (2)$$

where the system Hamiltonian

$$\mathcal{H} = - (1/2m^*) \nabla^2 + \mathcal{V}(x,y),$$

$\nabla^2$  is the Laplacian operator,  $\mathcal{V}(x,y)$  is the interaction potential, and  $m^* = 0.066m_e$  is the effective mass for GaAs.<sup>12</sup>

To solve the time-dependent Schrödinger equation, the Chebyshev method is used to approximate the exponential operator with a fast Fourier transform scheme to evaluate the action of the Laplacian operator. This has been proven to

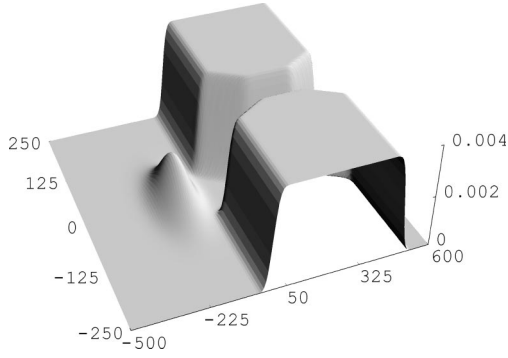


FIG. 1. Confinement potential and initial wave packet used in the calculations. The wave packet has been scaled to make it visible.

provide a highly efficient and accurate method to study such two-dimensional devices.<sup>11,13,14</sup>

The Chebyshev method approximates the exponential time propagator by a Chebyshev polynomial expansion<sup>15</sup>

$$\psi(x, y, t) = \exp[-i(\mathcal{E}_{max} + \mathcal{E}_{min})t] \times \sum_{n=0}^{\mathcal{N}} a_n(\alpha) \phi_n(-\tilde{\mathcal{H}}) \psi(x, y, 0), \quad (3)$$

where  $\mathcal{E}_{min}$  and  $\mathcal{E}_{max}$  are the minimum and maximum energy eigenvalues,  $a_n(\alpha) = 2J_n(\alpha)$  except for  $a_0(\alpha) = J_0(\alpha)$ ,  $J_n(\alpha)$  are the Bessel functions of the first kind,  $\phi_n$  are the Chebyshev polynomials, and the normalized Hamiltonian is defined as

$$\tilde{\mathcal{H}} = (1/\mathcal{E}_{max} - \mathcal{E}_{min}) [2\mathcal{H} - (\mathcal{E}_{max} + \mathcal{E}_{min})]. \quad (4)$$

This propagation scheme works for arbitrarily long time steps, and it is often referred to as a long-time propagator. We examine the electron wave propagation until the final wave packet has emerged from the interaction region in real space. In momentum space, the positive and negative part of the wave function will then be well separated, representing the transmission and reflection, respectively.

An example confinement potential  $\mathcal{V}(x, y)$  is shown in Fig. 1, together with the initial electron wave packet before entering the quantum wire. The flange shown here has an angle of  $18^\circ$  and the wire width is 46.6 nm. The amplitude of the wave packet was scaled to be visible on the graph with the potential. The potential walls are of finite height, but they are significantly higher than the incident energy of the incoming electron. As a result, leakage from the potential barriers is negligible. For the calculations presented in this paper, the potential height is typically 0.11 eV and the incident energy typically 0.054 eV with a 5% spread, corresponding to a temperature of approximately 3 K.

Calculations were carried out for a range of flange angles (from  $5^\circ$  to  $85^\circ$ ) and wire widths (from 14.8 to 46.6 nm). The length of the wire was 211.7 or 106 nm, and the length of the flanges was 106 nm for the results presented in this paper. It was found that the transmission behavior did not change when a longer or shorter wire was examined. The structures studied here are approximately an order of magni-

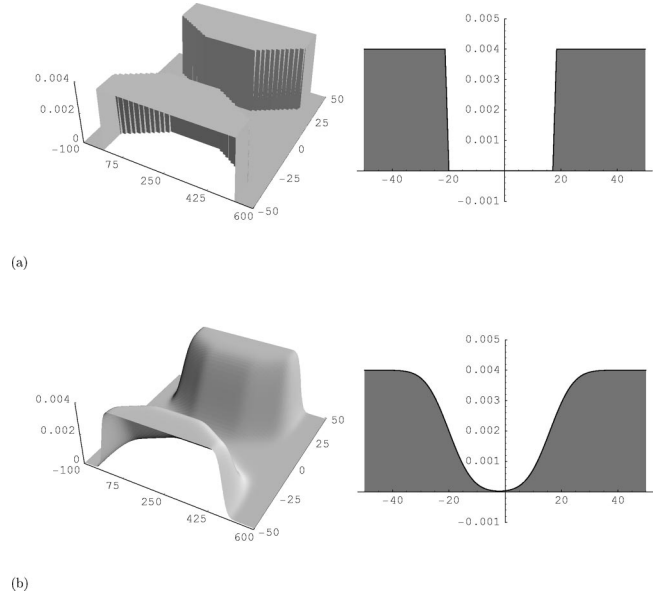


FIG. 2. Hard-wall potential and smooth-wall potential (with cross section through 250 nm) for the same flange angle. The smooth-wall potential represents more realistically a physical device.

tude smaller than those examined experimentally by Kane *et al.*<sup>16</sup> Nevertheless, the underlying physics at work should be the same. Transmission coefficients are obtained by integrating the transmitted wave packets in the region right of the quantum wire. Great care was taken to ensure that numerical error was minimized. A detailed error analysis of such a numerical scheme was given in Ref. 11. We also made sure that the final wave packet has emerged from the interaction region and the calculated transmission coefficients are independent of the propagation time.

Calculations were carried out using smooth-wall potentials as opposed to hard-wall potentials (see Fig. 2). The geometry used in the calculations is similar to those shown in Kane *et al.*<sup>16</sup> and Sohn *et al.*<sup>17</sup> The smooth-wall potentials are closer to reality as demonstrated, for example, from self-consistent calculation.<sup>18</sup> Such smooth-wall potentials cannot be easily dealt with using time-independent methods, as the boundary conditions are difficult to implement. However, the time-dependent approach we employed in this work treats the system as an initial value problem, and thus arbitrarily complex potentials can be readily implemented. A detailed discussion of the advantages in using the time-dependent approach against the conventional time-independent approaches was given in a previous paper.<sup>11</sup>

It is found that we are able to reproduce the conductance quantization as observed experimentally<sup>19,16</sup> and predicted theoretically<sup>19,9,8</sup> as shown in Fig. 3. The conductance was computed using the Landauer formula

$$G = (2e^2/h) NT, \quad (5)$$

where  $N = \text{Int}[2W/\lambda_f]$  is the integer number of modes across the quantum wire,  $\lambda_f$  is the Fermi wavelength,  $T$  is the transmission, and  $W$  is the width of the wire.<sup>20</sup>

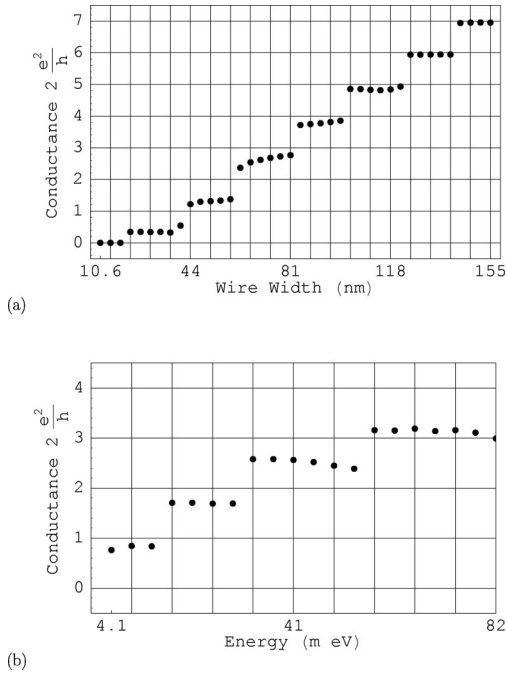


FIG. 3. (a) Conductance as the width of the wire increases and (b) conductance as the energy of the electron increases.

The results shown in Fig. 3(a) were calculated for a wire of 211.7 nm in length and flange angle of 18° with an incident energy of 0.054 eV, corresponding to a Fermi wavelength  $\lambda_f \approx 21$  nm. As expected from previous studies, the conductance changes as a stepping function with respect to the wire width. The results shown in Fig. 3(b) were calculated for a wire 106 nm in length, 18° of flange angle, and constant width of 100 nm. Again, we obtained quantized conductance including a diplike structure between adjacent plateaus, as observed by Csontos and Xu.<sup>8</sup>

In our calculation, the initial electron wave function is a Gaussian wave packet with a small spread in its energy (approximately 5%). As the wave packet enters the quantum wire, components of the wave packet will propagate through different available channels. As the central momentum aligns with a particular channel, a slight peak in transmission is

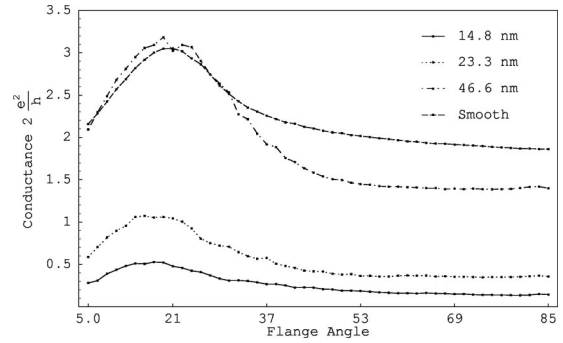


FIG. 4. Conductance for different flange angles from 5° to 85°. Results for three different wire widths are shown: 14.8, 23.3, 46.6, and 46.6 nm with a smooth-wall potential.

observed, and as it moves away, a slight dip occurs. These effects are reflected in the conductance presented in Fig. 3 as they relate by Eq. (5).

The main focus of this work is on the behavior of electron transport in a two-dimensional nanowire with flanges of different angles. Shown in Fig. 4 are the calculated conductance as a function of flange angles for three different wire widths and a comparison for a width of 46.6 nm between hard-wall and smooth-wall potentials. The overall behavior is in agreement with our expectation. For example, if the flange angle is small (close to 0°), the structure is effectively a longer wire without flanges, while a large flange angle (close to 85°) characterizes a short wire without flanges. Consequently, their transmission properties should be similar. This is demonstrated by the results having roughly the same transmission probability for small angles and large angles. The results also show that a smoothed potential does not change the overall shape of the curve. Increasing the height of the potential (from 0.109 to 0.163 eV) does not alter the transmission coefficients in any way.

What is interesting is the fact that the maximum transmission does not occur at 45°, which this type of symmetry argument suggests. In fact, the flange angle in the nanowire fabricated by Kane *et al.*<sup>16</sup> is approximately 45°, reflecting probably the same instinctive expectation. We found that the

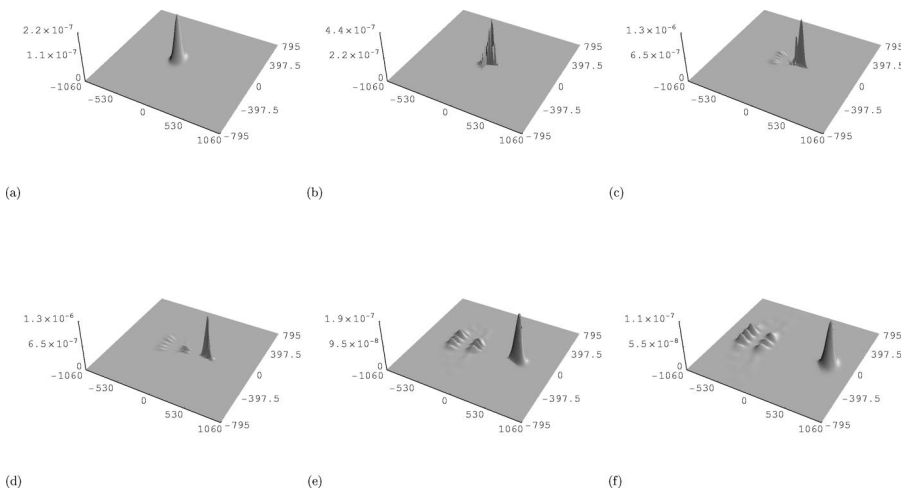


FIG. 5. Propagation of the electron wave packet for a flange angle of 18°. Top to bottom, left to right  $t=0, 0.356, 0.712, 1.068, 1.424,$  and  $1.78$  ps.

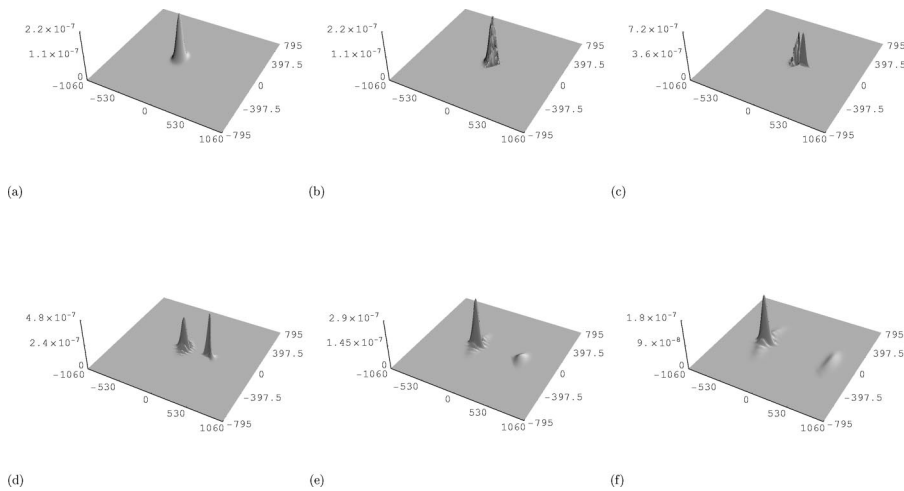


FIG. 6. Propagation of the electron wave packet for a flange angle of  $45^\circ$ . Top to bottom, left to right  $t=0, 0.356, 0.712, 1.068, 1.424,$  and  $1.78$  ps.

maximum transmission actually occurs at around  $18^\circ$  regardless of the wire width or length.

By looking at the actual propagation of the wave function for the maximum transmission case and comparing it to the case for a flange angle of  $45^\circ$ , an interesting observation is made (see Fig. 5 and Fig. 6). In the  $45^\circ$  case, the wave function has partial reflection from the flange and the wire as expected. However, in the maximum transmission case, it appears as though the wave packet first reflects from the flange and then resonantly reflects from the inlet after being trapped for a short period of time (in the order of 0.2 ps). Such resonance trapping allows the wave packet to readjust its momentum components and, as a result, enhances the overall transmission through the wire. With further study of this resonance behavior, additional increase in transmission may be achieved, perhaps even to 100%. To accomplish this, nonlinear-shaped flanges may need to be considered.

When the initial energy, the energy spread of the incoming wave packet, or the length of the flange is varied, the resonance condition changes. As a result, the optimal flange angle shifts slightly. For example, with double the initial energy (0.109 eV) the peak transmission moved about  $3^\circ$  to the left (i.e., smaller angle). Similarly with half the initial energy

(0.027 eV) the peak transmission moved about  $3^\circ$  to the right (i.e., larger angle). Likewise it was found that by varying the energy spread (i.e., the width of the Gaussian wave packet) in the range of 5–20%, corresponding to temperatures about 3–14 K, the optimal flange angle changes by a few degrees. When the length of the flange is doubled or halved, a shift of a few degrees in the optimal angle is also observed.

Our results follow from detailed numerical calculations, and the optimal flange angle is found to correspond to the resonant reflection and trapping observed in the actual propagation of the wave packet. Considering the experimental condition of Kane *et al.*, our study leads us to believe that if Kane *et al.* change the flange angle in their nanowire, an enhanced transmission will be observed.

In conclusion, this paper demonstrates that the way in which a nanowire is connected to the external electron source can greatly effect the transmission properties of the wire. With Fermi energy around 0.05 eV and a temperature of 3 K, the optimal flange angle for maximum transmission is found to be approximately  $18^\circ$  with a small shift due to a change in the initial energy, the energy spread of the electron, or the length of the flange.

<sup>1</sup>L. Sohn, Nature (London) **394**, 131 (1998).

<sup>2</sup>H. Wu, D.W.L. Sprung, and J. Martorell, Phys. Rev. B **45**, 11 960 (1992).

<sup>3</sup>*Mesoscopic Electron Transport*, edited by L. L. Sohn, L. P. Kouwenhoven, and G. Schön (Kluwer Academic, Dordrecht, 1997).

<sup>4</sup>C.C. Eugster *et al.*, Appl. Phys. Lett. **60**, 642 (1992).

<sup>5</sup>M. Hannan *et al.*, Superlattices Microstruct. **20**, 427 (1996).

<sup>6</sup>A. Bezryadin, C. Dekker, and G. Schmid, Appl. Phys. Lett. **71**, 1273 (1997).

<sup>7</sup>J.A.D. Alamo, C.C. Eugster, and Q. Hu, Superlattices Microstruct. **23**, 121 (1998).

<sup>8</sup>D. Csontos and H.Q. Xu, Appl. Phys. Lett. **77**, 2364 (2000).

<sup>9</sup>A. Szafer and A.D. Stone, Phys. Rev. Lett. **62**, 300 (1989).

<sup>10</sup>M. Rasavy, Int. J. Mod. Phys. B **11**, 2777 (1997).

<sup>11</sup>J.B. Wang and S. Midgley, Phys. Rev. B **60**, 13 668 (1999).

<sup>12</sup>C. Kittel, *Introduction to Solid State Physics* (Wiley, New York, 1986).

<sup>13</sup>J.B. Wang and T. Scholz, Phys. Rev. A **57**, 3554 (1998).

<sup>14</sup>S. Midgley and J.B. Wang, Phys. Rev. E **61**, 920 (2000).

<sup>15</sup>H. Tal-Ezer and R. Kosloff, J. Chem. Phys. **81**, 3967 (1984).

<sup>16</sup>B. Kane *et al.*, Appl. Phys. Lett. **72**, 3506 (1998).

<sup>17</sup>L. Sohn, L. P. Kouwenhoven, and G. Schön, *Mesoscopic Electron Transport* (Kluwer Academic, Dordrecht, 1996), pp. 5–6.

<sup>18</sup>S.E. Laux, D.J. Frank, and F. Stern, Surf. Sci. **196**, 101 (1988).

<sup>19</sup>B.J. van Wees *et al.*, Phys. Rev. Lett. **60**, 848 (1988).

<sup>20</sup>S. Datta, *Electronic Transport in Mesoscopic Systems* (Cambridge University Press, Cambridge, England, 1995).